X-621-70-108
PREPRINT

NASA TM X-63906

OBSERVATIONS OF THE SUPRATHERMAL ELECTRON FLUX AND THE ELECTRON TEMPERATURE AT HIGH LATITUDES

E. J. MAIER
B. C. NARASINGA RAO

MARCH 1970

GSFC — GODDARD SPACE FLIGHT CENTER
GREENBELT, MARYLAND

OBSERVATIONS OF THE SUPRATHERMAL ELECTRON FLUX AND THE ELECTRON TEMPERATURE AT HIGH LATITUDES

by

E.J. Maier and B.C. Narasinga Rao†
Laboratory for Planetary Atmospheres
NASA, Goddard Space Flight Center
Greenbelt, Maryland, U.S.A.

ABSTRACT

Observations of suprathermal electrons in the energy range of 5-200 eV were obtained with retarding potential analysers on Explorer 31 in the altitude range of 1700 to 3000 km over the northern high latitudes during winter 1965-1966. It is found that there are three distinct zones consisting mainly of (i) a steady flux of photoelectrons in the midlatitudes (ii) a high and variable flux containing precipitated particles in the auroral latitudes and (iii) a low flux over the polar region. Evidence is presented to show that the magnetic field lines are closed at least up to L = 7.7 for these particles. The boundaries of precipitation vary with local time and are somewhat different from those of the auroral oval. The ambient electron temperature appears to be dependent on the level of flux in the auroral and polar region.

†NRC-NASA Resident Research Associate on leave from the National Physical Laboratory, New Delhi, India

INTRODUCTION

In recent years observations of energetic electrons precipitating over high latitudes have been extended to lower energies (Evans et al 1967; Burch, 1968; Hoffman, 1969). These measurements in the topside ionosphere and magnetosphere were made with polar orbiting satellites and the energies were extended down to about 50 eV. They indicate the existence of a region of precipitation over the auroral zone, but extending poleward of the auroral oval and characterized by spectral softening and rapid temporal and/or spatial variation. This region has been described as a 'soft' zone (Burch, 1968) or 'burst' zone (Hoffman, 1969). One of the important effects of the incidence of these low energy electrons on the earth's upper atmosphere is the production of ionization at F region levels and above (Maehlum, 1968; 1969; Burch, 1969; and Rees, 1969). The high latitude termination of the flux near the magnetic pole appeared to be responsible for the low level of F region ionization and also of 6300 Å intensity (Maehlum, 1969; Eather, 1969). In the present paper we report high latitude observations from Explorer 31 of still lower energy electrons in the range of 5 eV to 200 eV, which may be referred to as suprathermal electrons or eV-range electrons. Extension of the spectrum to such low energies will help in understanding the temperature behavior of the ambient electrons, since the eV range electrons are more efficient in heating the ambient electrons. Our measurements refer to the total flux of the precipitating or escaping (primary and secondary) low energy electrons and to the ionospheric photoelectrons, which are also in the same energy range.

MEASUREMENT TECHNIQUES

The present measurements are made with retarding potential analysers aboard Explorer 31, whose perigee is 500 km and apogee 3000 km and which is spinning at a nominal period of 20 seconds. There are three sensors which are referred to as the (1) electron sensor, (2) ion sensor and (3) energetic electron sensor. They consist of multigrid traps with a collector and a ramp grid whose voltage is swept in the proper voltage range. The schematic diagrams are shown in Fig. 1. The details of their operation are described by Donley (1969) and Maier (1969). While sensor 1 and sensor 2 are designed mainly to measure temperatures and densities of thermal electrons and ions, sensor 3 is designed to measure the energetic electron fluxes at different threshold energies varying from about 2 volts to 200 volts. However, sensor 1 can also measure the integral flux of all electrons with energies greater than 5 eV and sensor 2 can measure the integral flux of all electrons with energies greater than 15 eV. In this paper we present the observations both in terms of integral fluxes as well as differential energy spectra. These observations are made during the winter months of 1965-66 over the northern high latitudes in the altitude range of 1700-3000 km.

CHARACTERISTIC FEATURES OF HIGH LATITUDE FLUXES

Fig. 2 illustrates some typical observations made during a pass covering both auroral and polar latitudes. Under the X axis are shown the Universal time, the magnetic latitude, McIlwain parameter L, and the solar zenith angle χ at the location of the satellite. The parameter L is obtained from a spherical harmonic expansion of the main geomagnetic field. The Y axis shows the energetic electron flux per square centimeter per second. The integral fluxes of electrons above 5 eV are obtained from sensor 1 and those above 7 eV are obtained from sensor 3; both are plotted in the figure to demonstrate that they give essentially the same variation. In the following, fluxes from sensor 1 are used to describe various features of high latitude phenomena since more frequent observations are available from this sensor, and the fluxes from sensor 3 are used mainly for deriving differential energy spectra since it gives fluxes at different threshold energies. Referring to Fig. 2 we find a fairly steady flux up to magnetic latitude of 68^{o}, then a large increase with irregular structure up to 76^{o} and a lower flux over the polar region above 80^{o}. From this figure three zones may be defined: (i) steady zone, (ii) high flux zone and (iii) low flux zone. They correspond approximately to the midlatitude zone, the auroral zone and the polar zone respectively. As mentioned in the introduction the measured fluxes consist of ionospheric photoelectrons escaping upward from the F region production levels, any possible precipitated electrons from the magnetosphere, and any resulting secondaries. At first, it may appear feasible to identify these two types by looking up or down the field line, but it should be realized that scattering effects and the production of secondaries will complicate the angular distribution. In fact, the observed pitch angle distribution, within the limits of the present technique, shows a more or less isotropic distribution. Therefore, we used the variation in the intensity levels as the criteria to distinguish the precipitated particles from the photoelectrons. The photoelectron flux is dependent on the solar zenith angle χ, the level being fairly constant for χ values ranging from 80^{o} - 0^{o}, while the precipitation flux (which includes primaries and secondaries) shows more variability with time and/or space. Using the above criteria, we find from Fig. 2 that the steady flux in the mid-latitude zone may be attributed to the ionospheric photoelectrons alone since this is the level normally observed both at low and mid-latitudes when both ends of the field line are sunlit. The higher level and greater variability in flux in the auroral zone indicate that there are appreciable numbers of precipitated particles in addition to photoelectrons.

In the above figure the zonal behavior of the integral flux is shown. However, it is necessary to know the differential energy distribution to establish that these levels really reflect flux levels of low energy electrons.

In Fig. 3 the differential energy spectra are shown separately for each zone. On the left are shown the spectra of the steady photoelectron flux, in the middle the high flux, and on the right the low flux. It is immediately clear that the levels of the integral fluxes noted earlier in the three zones are reflected in the differential fluxes of low energy particles. For example, the flux of 10 eV particles is high in the high flux zone and low in the low flux zone. Therefore the integral flux levels for E > 5 eV can be taken as indicative of the fluxes of low energy electrons.

From Fig. 3 it may be noted that the spectral shapes are also different in the three zones. In the mid-latitude zone the shapes are very uniform and resemble the spectrum of photoelectrons observed at lower latitudes. In the auroral zone the spectral shape becomes highly variable. There is also a trend towards a second peak around 100 eV. In the polar zone the shapes are relatively less variable with a slow decrease of flux with increasing energy.

CLOSED FIELD LINE BOUNDARY FOR THE LOW ENERGY ELECTRONS

It was mentioned earlier that in the mid-latitude zone the observed flux consists mainly of ionospheric photoelectrons. Since their production is controlled by the incidence of solar radiation, during the predawn period they will be observed at the time of conjugate point sunrise, if the geomagnetic field lines are closed as in the case of lower latitudes (Rao and Maier, 1970). Thus, the incidence of conjugate photoelectrons can be used as a test for finding the closed field line boundary. Fig. 4 shows high latitude observations in the northern hemisphere at the time of conjugate sunrise. This pass covers from 53^o to

64^{o} magnetic latitude and L values from 4 to 7.7. The solar zenith angles at both ends of the field lines at the 300 km level (χ_L in the local ionosphere and χ_c in the conjugate ionosphere) are also shown under the χ axis. For this pass the local ionosphere is in darkness as can be seen from χ_L and sunrise is taking place in the conjugate ionosphere since χ_c is varying from 96^{o} to 87^{o}.

During this period the flux shows a gradual increase reaching almost a steady value. The smooth increase of flux during the conjugate sunrise indicates that these are the photoelectrons coming from the conjugate hemisphere. Since this behavior is observed up to L = 7.7 it is reasonable to conclude that the field lines are closed at least up to this L value during night-time (MLT = 0130 hrs.). Beyond the closed field line boundary there will be a drop in the flux where the field lines become open. However, it is found that there is also precipitation from the magnetosphere superposed on the photoelectron flux making it impossible to locate the drop in the photoelectron flux. Therefore, this technique has yielded only the lower limit on the boundary for the closure of field lines as tested by the South to North propagation of low energy electrons. This lower limit of L = 7.7 and 64^{o} magnetic latitude lies within the boundary (69^{o} mag. lat.) determined by Fairfield (1968) from the magnetic field measurements at local midnight. In this connection it may be pointed out that Bennett (1969) determined the limits over which the intervening magnetospheric domain permits the photoelectrons to propagate from one hemisphere to the other from a study of 6300 Å airglow predawn enhancements at a few stations. He found a limit of L = 3.2 and inferred that this upper limit is imposed by magnetospheric electric fields of such magnitude and direction as to preclude propagation of the low energy conjugate photoelectrons. However, from the present direct observations, we find that the conjugate photo-electrons, can reach the other hemisphere up to L = 7.7. This can be interpreted to mean that the electric fields are not of sufficient magnitude or direction to significantly perturb them up to this L value.

DEPENDENCE OF THE PRECIPITATION ZONE BOUNDARY ON MAGNETIC LOCAL TIME

From a study of a large number of passes, it is found that the boundaries of the zones of precipitated particles depend on the magnetic local time. Before presenting the data for different times the main differences are first illustrated with a typical daytime pass and a typical night time pass which are shown in Figs. 5a and 5b respectively. During daytime (Fig. 5a) the steady photoelectron flux continues up to magnetic latitude 75°, and precipitation occurs beyond that latitude. In contrast to this, at nightime, precipitation starts at a much lower latitude. At night (Fig. 5b), from 60° onwards, the flux is variable and larger than the steady photoelectron flux level indicating that there is precipitation even at a latitude of 60°. In fact, at the beginning of the pass the flux is wholly due to precipitation since both χ_L and χ_c are greater than 96^o (note from Fig. 4 that the photoelectron flux from the conjugate hemisphere would be less than 10^8 el cm^{-2} sec^{-1} for $\chi_c > 95^o$). After showing the major difference in the lower boundary of the precipitation zone between day and night, the variation of the lower and upper boundaries of this zone with magnetic local time are shown in Fig. 6. In this polar diagram the coordinates are geomagnetic latitude and magnetic local time (MLT). Observations from a number of passes during the period Dec. 1965 to Feb. 1966 are included to cover all the magnetic local times. The observations are denoted by three symbols based on the photoelectron flux which is normally between 2-3 x 10^8 el cm^{-2} sec^{-1}. A slightly higher value than this, i.e. 4 x 10^8 el cm^{-2} sec^{-1} is chosen as upper boundary and a slightly lower value of 1 x 10^8 el cm^{-2} sec^{-1} is chosen as lower boundary. If the flux is higher than the upper boundary precipitation is considered to be present and if it is less than the lower boundary it is considered to be absent. The definition of the precipitation in this manner may not be accurate, but is considered reasonably indicative for the present purpose. The high latitude boundary for eV electrons lies at about 80^o in the dayside and 70^o in the nightside. The low latitude boundary lies at about 70^o-74^o in the dayside and 55-60^o in the nightside. For comparison, we have also shown in Fig. 6 the boundaries of the auroral oval as given by Hartz and Brice (1967) which are based on the frequency of incidence of various types of auroral phenomena, including short duration bursts of < 20 Kev electrons and discrete auroral forms (Feldstein, 1966). It appears that, compared to the auroral oval, the boundaries extend towards the pole in the dayside and towards the midlatitudes in the nightside.

EFFECTS OF EV ELECTRON FLUX ON THE HIGH LATITUDE BEHAVIOR OF IONOSPHERIC ELECTRON TEMPERATURES.

The low energy electrons are very efficient in heating the ambient electrons through elastic collisions (Dalgarno et al, 1963). Therefore, it is natural to expect that the fluxes of these precipitating low energy electrons strongly influence the electron temperature in these high latitudes. Fortunately, we have simultaneous observations of the electron temperature, as determined by sensor 1, allowing us to study T_e in relation to the fluxes. Fig. 7 illustrates the typical behavior of both the flux variation and the T_e variation. At midlatitude $T_e \approx 4000^o$ which is the normal value observed under sunlit condition at these latitudes; i.e., the value of T_e under the incidence of the photoelectron flux. Figure 7 shows that northward T_e increases rapidly towards the region of high flux. Within the high flux region precise T_e measurements could not be made because of the interference of suprathermal particles in the electron current retardation curves of sensor 1. However, the nature of the retardation curves indicate a high temperature. North of the high flux zone, towards the magnetic pole, T_e decreases from a value of about 8000 ^oK to about 4000 ^oK in the polar region corresponding to the decrease in flux. Thus, the decrease of T_e in the polar region appears to be caused by the decrease in the suprathermal flux. On the other hand, in the midlatitude region, T_e increases before the flux increases.

We have shown in a recent paper (Rao and Maier, 1970) that significant backscattering and/or mirroring of the suprathermal particles occur within the protonosphere. It is suggested that this coupling, plus possible wave interaction, can serve to inject electrons into orbits where they mirror above about 1500 km. It is possible that the proprotion of thermal electrons scattering into such pseudo-trapped orbits may increase with L shell. Thus, the increase of temperature with latitude may result from an increased number of electrons in pseudo-trapped orbits storing heat energy in the magnetosphere.

In summary we may state that observations of suprathermal (eV energy) electron fluxes show three distinct zones consisting mainly of (I) steady photoelectron fluxes in midlatitudes (II) high and variable fluxes of precipitating (including secondaries) particles in the auroral zone and (III) low fluxes in the polar zone. The boundaries of the precipitation zone are somewhat different from the auroral boundaries as determined by the precipitation of KeV particles. Finally, the ambient electron temperatures in the auroral and polar regions appear to be controlled by the intensity of the flux of suprathermal electrons.

REFERENCES

1. Bennett, R.E., Latitude dependence of 6300 A (OI) twilight airglow enhancement, J. Geophys. Res., 74, 381, 1969.
2. Burch, J.L., Low energy electron fluxes at latitudes above the auroral zone, J. Geophys. Res., 73, 3585, 1968.
3. Burch, J.L., Satellite measurements of low energy electrons precipitated at high latitudes, paper presented at the NATO Advanced Study Institute," Production and Maintenance of the Polar Ionosphere", Tretten, Norway, April 9-18, 1969.
4. Dalgarno, A., M.B. McElroy, and R.J. Moffett, Electron temperatures in the ionosphere, Planet. Space Sci., 11, 463, 1963.
5. Donley, J.L., The thermal ion and electron trap experiments on the Explorer 31 Satellite, Proc. IEEE, 57, 1061, 1969.
6. Eather, R.H., Latitudinal distribution of auroral and airglow emissions: The soft auroral zone, J. Geophys. Res., 74, 153, 1969.
7. Evans, J.E., R. G. Johnson, R.D. Sharp, and J.B. Reagan, Recent results from satellite measurements of low energy particles precipitated at high latitudes, Space Sci. Rev., 7, 263, 1967.
8. Fairfield, D.H., The average magnetic field configuration of the outer magnetosphere, J. Geophys. Res., 73, 7329, 1968.

9. Feldstein, Y.I., Peculiarities in the auroral distribution and magnetic disturbance distribution in high latitudes cuased by the asymmetrical form of the magnetosphere, Planet. Space Sci., 14, 121, 1966.

10. Hartz, T.R., and N.M. Brice, The general pattern of auroral particle precipitation, Planet. Space Sci., 15, 301, 1967.

11. Hoffman, R.A., Low energy electron precipitation at high latitudes, J. Geophys. Res. 74, 2425, 1969.

12. Maehlum, B.N., Universal-time control of the low energy electron fluxes in the polar regions, J. Geophys. Res., 74, 3459, 1968.

13. Maehlum, B.N., On the high latitude, Universal time controlled F-layer, J. Atmosphr. Terr. Phys. 31, 531, 1969.

14. Maier, E.J.R., Explorer 31 total current monitor experiments, Proc. IEEE, 57, 1068, 1969.

15. Rao, B.C.N., and E.J.R. Maier, Photoelectron flux and protonospheric heating during the conjugate point sunrise, J. Geophys. Res., 75, 816, 1970.

16. Rees, M.H., Effects of low energy electron precipitation on the upper atmosphere, paper presented at the NATO Advanced Study Institute","Production and Maintenance of the polar ionosphere", Tretten, Norway, April 9-18, 1969.

FIGURE CAPTIONS

Fig. 1. Schematic diagrams of the three planar grided retarding potential analysers on Explorer 31.

Fig. 2. High latitude variation of integral electron fluxes illustrating the presence of three flux zones.

Fig. 3. Differential energy spectra of the suprathermal electrons in the three zones.

Fig. 4. Latitudinal variation of the electron flux during conjugate sunrise.

Fig. 5. Latitudinal variations of the integral electron flux during daytime (Local time 12:40 to 14:30 hrs., Fig. 5a) and during night time (Local time 03:10 to 04:15 hrs., Fig. 5b).

Fig. 6. Dependence of the precipitation zone boundaries on magnetic local time. The individual passes are labelled with the month, day, hour and minute in U.T. of the start of the pass. The data presented were obtained from December 6, 1965 through March 5, 1966.

Fig. 7. Simultaneous observations of the suprathermal electron flux and the ambient electron temperature.

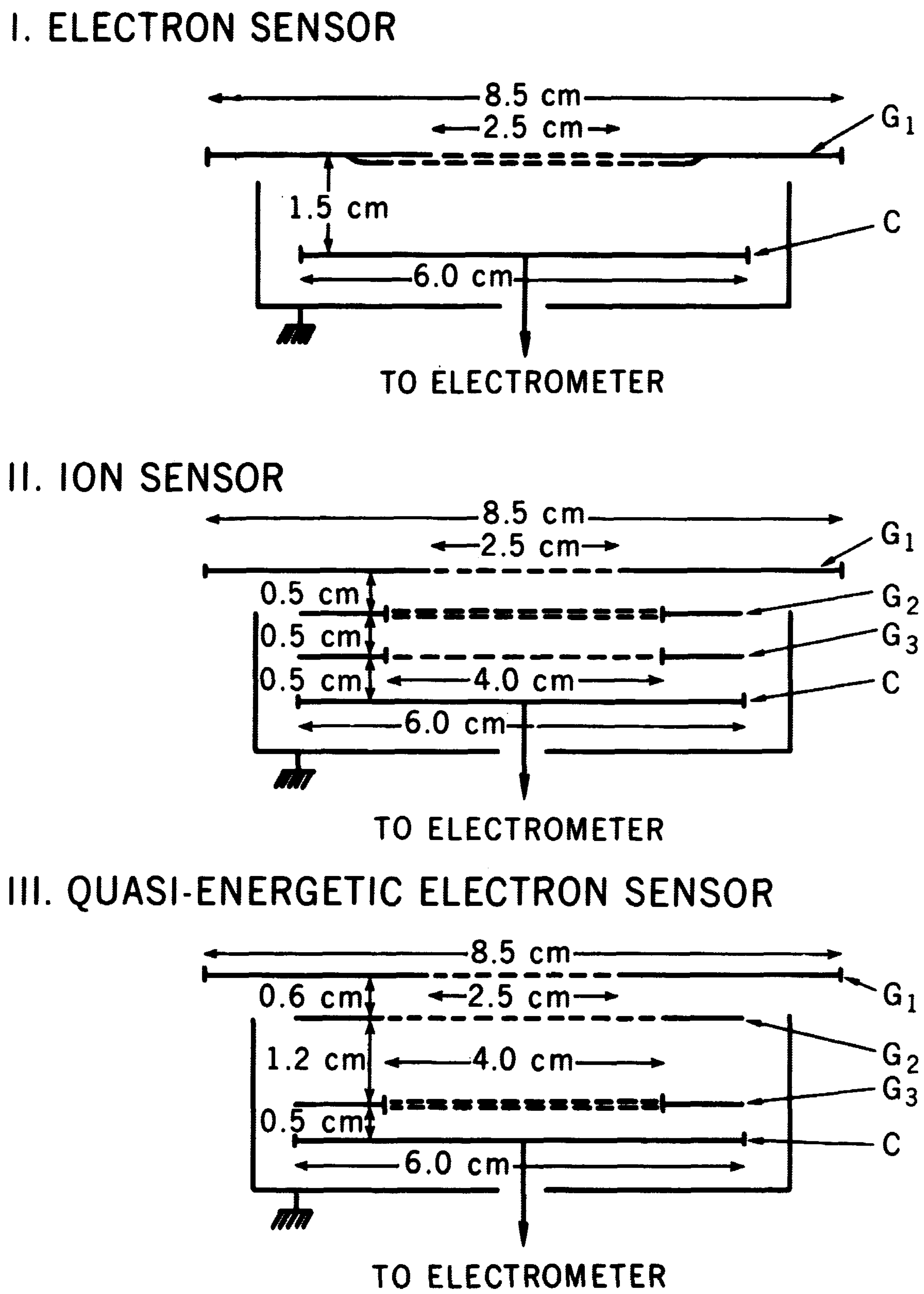
I. ELECTRON SENSOR
8.5 cm
2.5 cm
G1
1.5 cm
C
6.0 cm
TO ELECTROMETER
II. ION SENSOR
8.5 cm
2.5 cm
G1
0.5 cm
G2
0.5 cm
G3
0.5 cm
4.0 cm
C
6.0 cm
TO ELECTROMETER
III. QUASI-ENERGETIC ELECTRON SENSOR
8.5 cm
0.6 cm
2.5 cm
G1
1.2 cm
4.0 cm
G2
G3
0.5 cm
C
6.0 cm
TO ELECTROMETER

Figure 1

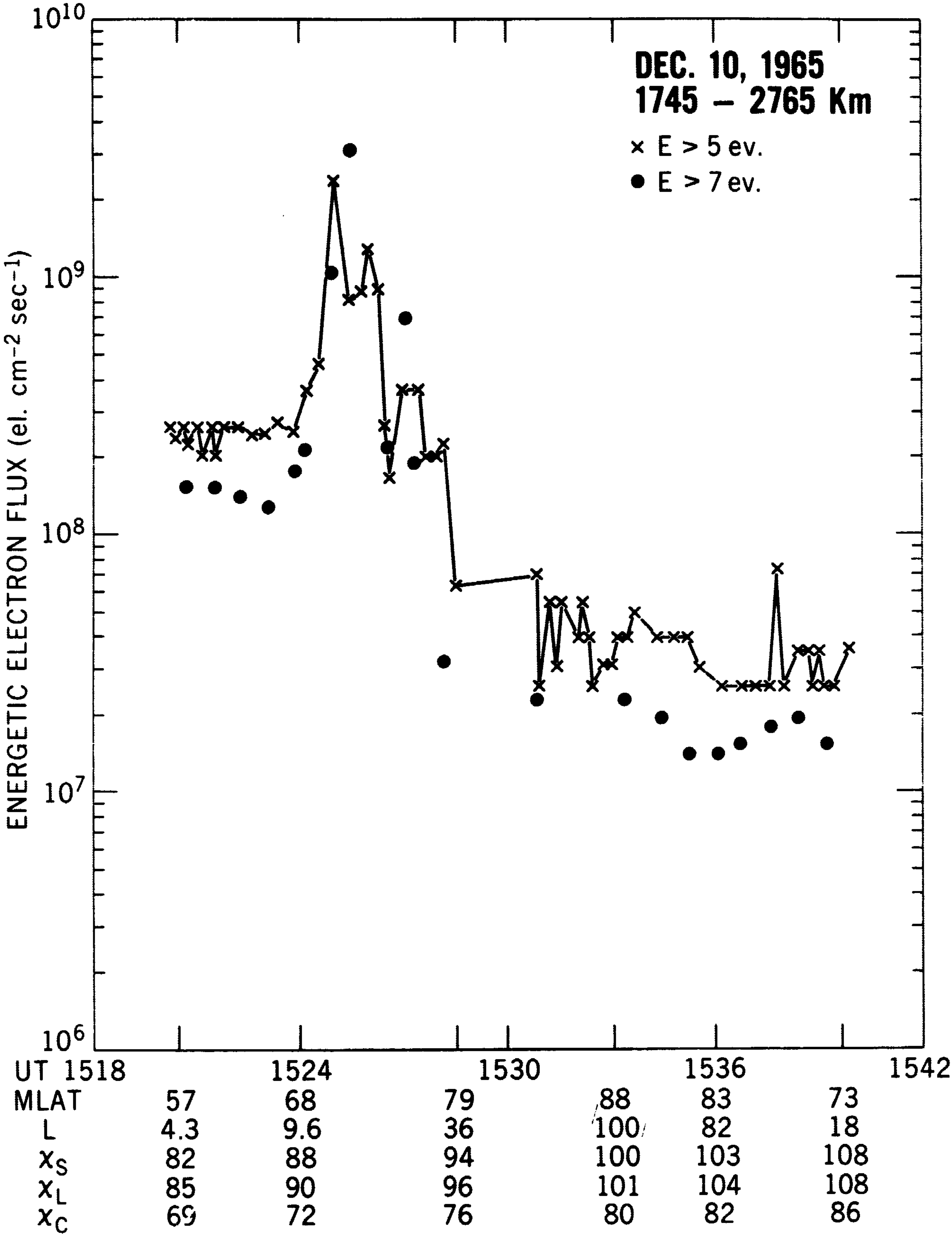
DEC. 10, 1965
1745 – 2765 Km
× E > 5 ev.
● E > 7 ev.
ENERGETIC ELECTRON FLUX (el. cm⁻² sec⁻¹)
10^10
10^9
10^8
10^7
10^6
UT 1518 1524 1530 1536 1542
MLAT 57 68 79 88 83 73
L 4.3 9.6 36 100 82 18
χS 82 88 94 100 103 108
χL 85 90 96 101 104 108
χC 69 72 76 80 82 86

Figure 2

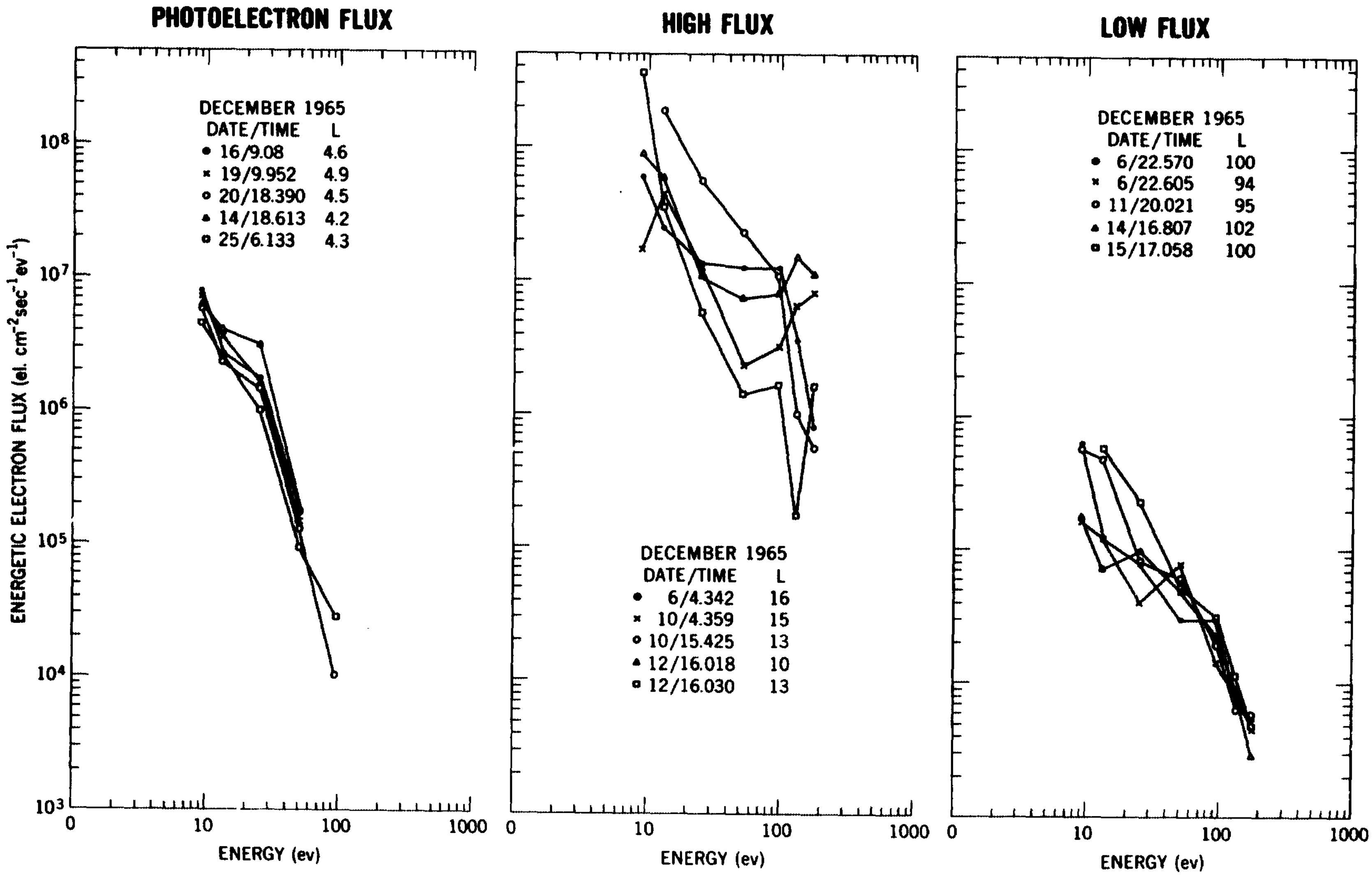
PHOTOELECTRON FLUX
DECEMBER 1965
DATE/TIME L
• 16/9.08 4.6
× 19/9.952 4.9
○ 20/18.390 4.5
▲ 14/18.613 4.2
□ 25/6.133 4.3
HIGH FLUX
DECEMBER 1965
DATE/TIME L
• 6/4.342 16
× 10/4.359 15
○ 10/15.425 13
▲ 12/16.018 10
□ 12/16.030 13
LOW FLUX
DECEMBER 1965
DATE/TIME L
• 6/22.570 100
× 6/22.605 94
○ 11/20.021 95
▲ 14/16.807 102
□ 15/17.058 100
ENERGETIC ELECTRON FLUX (el. cm^{-2}sec^{-1}ev^{-1})
ENERGY (ev)
10^3
10^4
10^5
10^6
10^7
10^8
0
10
100
1000

Figure 3

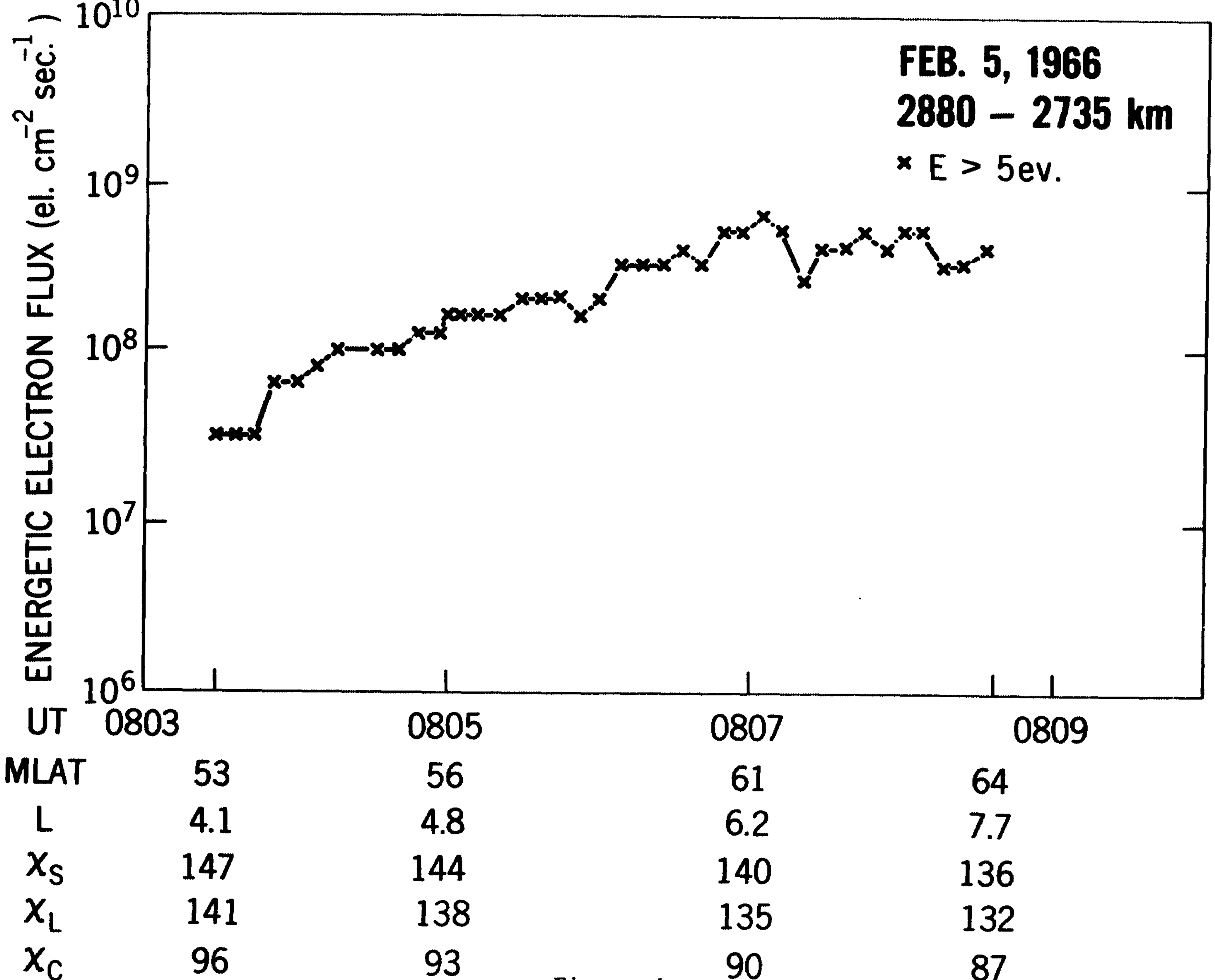
FEB. 5, 1966
2880 – 2735 km
× E > 5ev.
ENERGETIC ELECTRON FLUX (el. cm⁻² sec.⁻¹)
10^10
10^9
10^8
10^7
10^6
UT 0803 0805 0807 0809
MLAT 53 56 61 64
L 4.1 4.8 6.2 7.7
χS 147 144 140 136
χL 141 138 135 132
χC 96 93 90 87

Figure 4

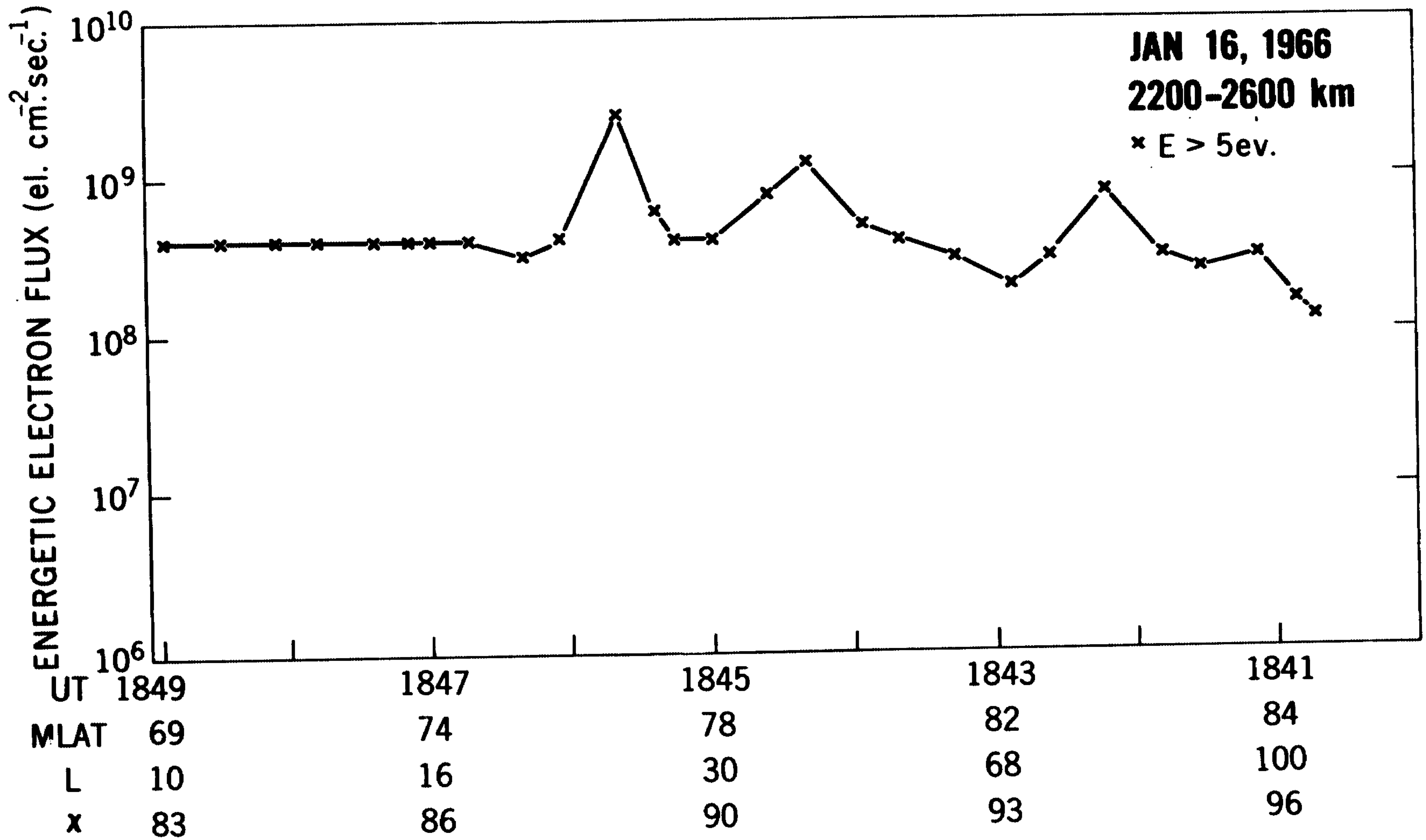
ENERGETIC ELECTRON FLUX (el. cm.-2 sec.-1)
10^10
10^9
10^8
10^7
10^6
JAN 16, 1966
2200-2600 km
× E > 5ev.
UT 1849 1847 1845 1843 1841
MLAT 69 74 78 82 84
L 10 16 30 68 100
x 83 86 90 93 96

Figure 5a

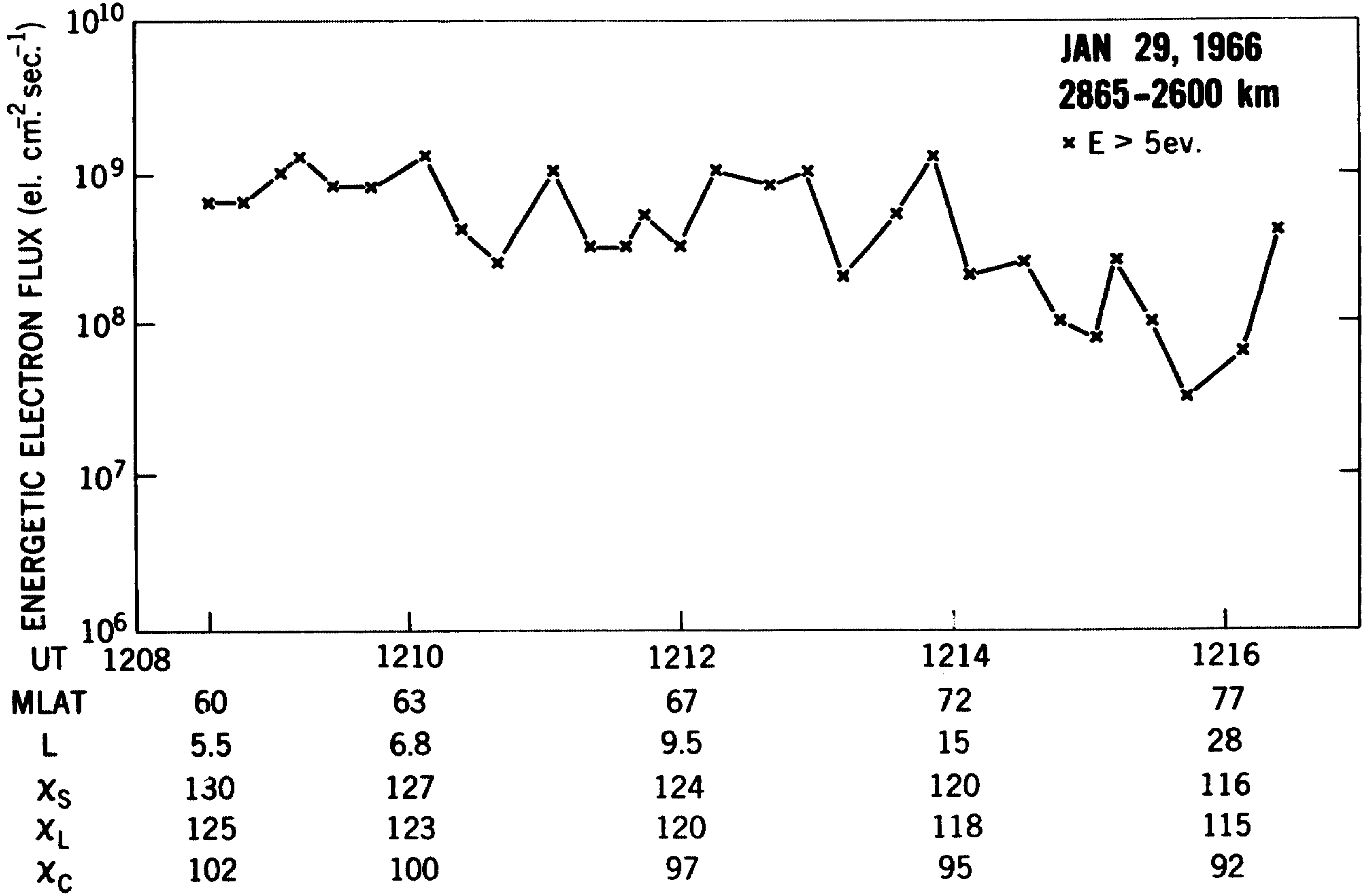
JAN 29, 1966
2865-2600 km
× E > 5ev.
ENERGETIC ELECTRON FLUX (el. cm⁻² sec⁻¹)
10¹⁰
10⁹
10⁸
10⁷
10⁶
UT 1208 1210 1212 1214 1216
MLAT 60 63 67 72 77
L 5.5 6.8 9.5 15 28
Xs 130 127 124 120 116
XL 125 123 120 118 115
Xc 102 100 97 95 92

Figure 5b

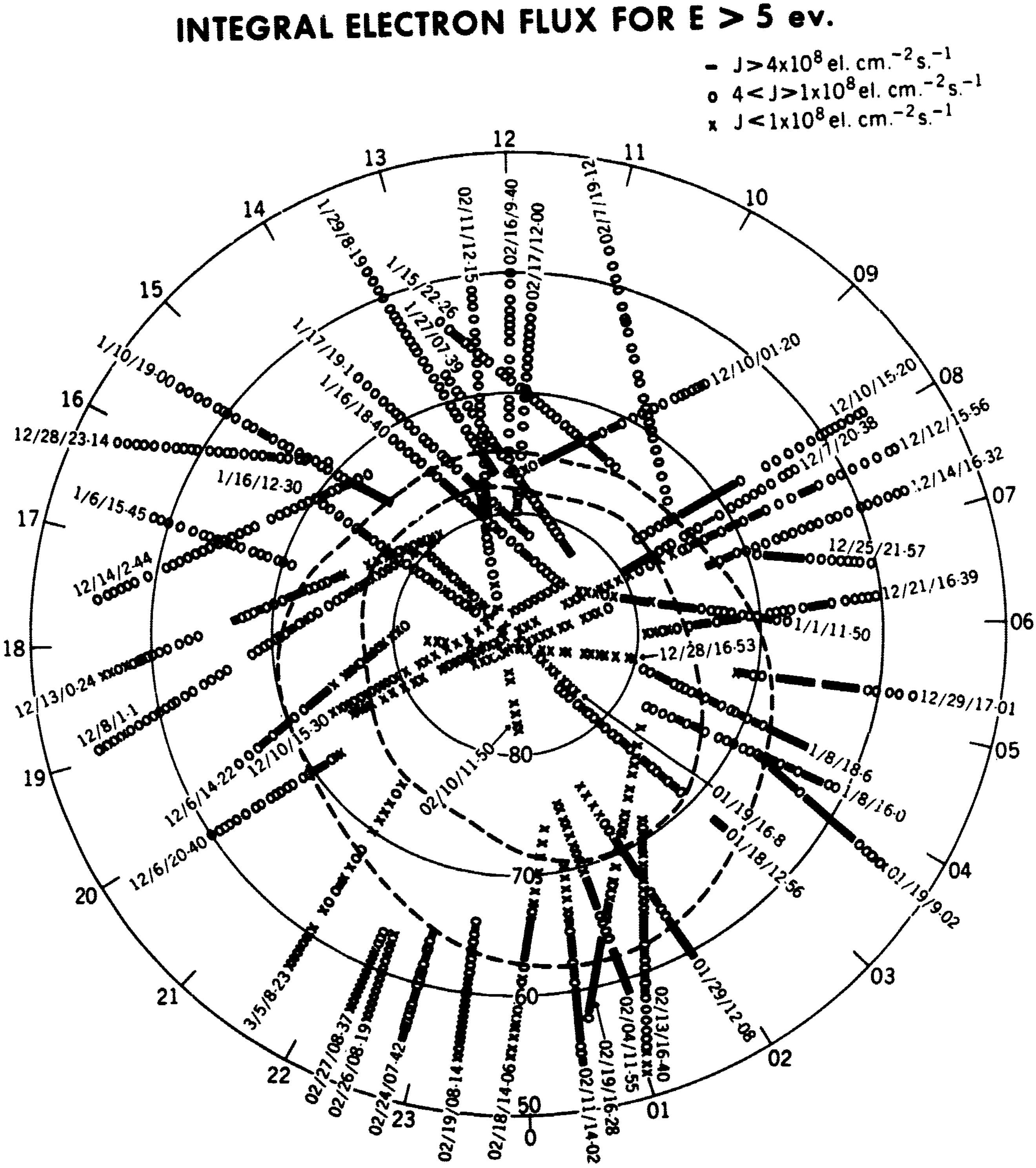
INTEGRAL ELECTRON FLUX FOR E > 5 ev.
- J>4x10^8 el. cm.^-2 s.^-1
o 4<J>1x10^8 el. cm.^-2 s.^-1
x J<1x10^8 el. cm.^-2 s.^-1
12
11
10
09
08
07
06
05
04
03
02
01
0
23
22
21
20
19
18
17
16
15
14
13
80
70
60
50
02/11/12-15
02/16/9-40
02/17/12-00
02/7/19-12
1/29/8-19
1/15/22-26
1/27/07-39
1/17/19-1
1/16/18-40
1/10/19-00
12/28/23-14
1/16/12-30
1/6/15-45
12/14/2-44
12/13/0-24
12/8/1-1
12/10/15-30
12/6/14-22
12/6/20-40
02/10/11-50
12/10/01-20
12/10/15-20
12/7/20-38
12/12/15-56
12/14/16-32
12/25/21-57
12/21/16-39
1/1/11-50
12/28/16-53
12/29/17-01
1/8/18-6
1/8/16-0
01/19/16-8
01/18/12-56
01/19/9-02
01/29/12-08
02/13/16-40
02/04/11-55
02/19/16-28
02/11/14-02
02/18/14-06
02/19/08-14
02/24/07-42
02/26/08-19
02/27/08-37
3/5/8-23

Figure 6

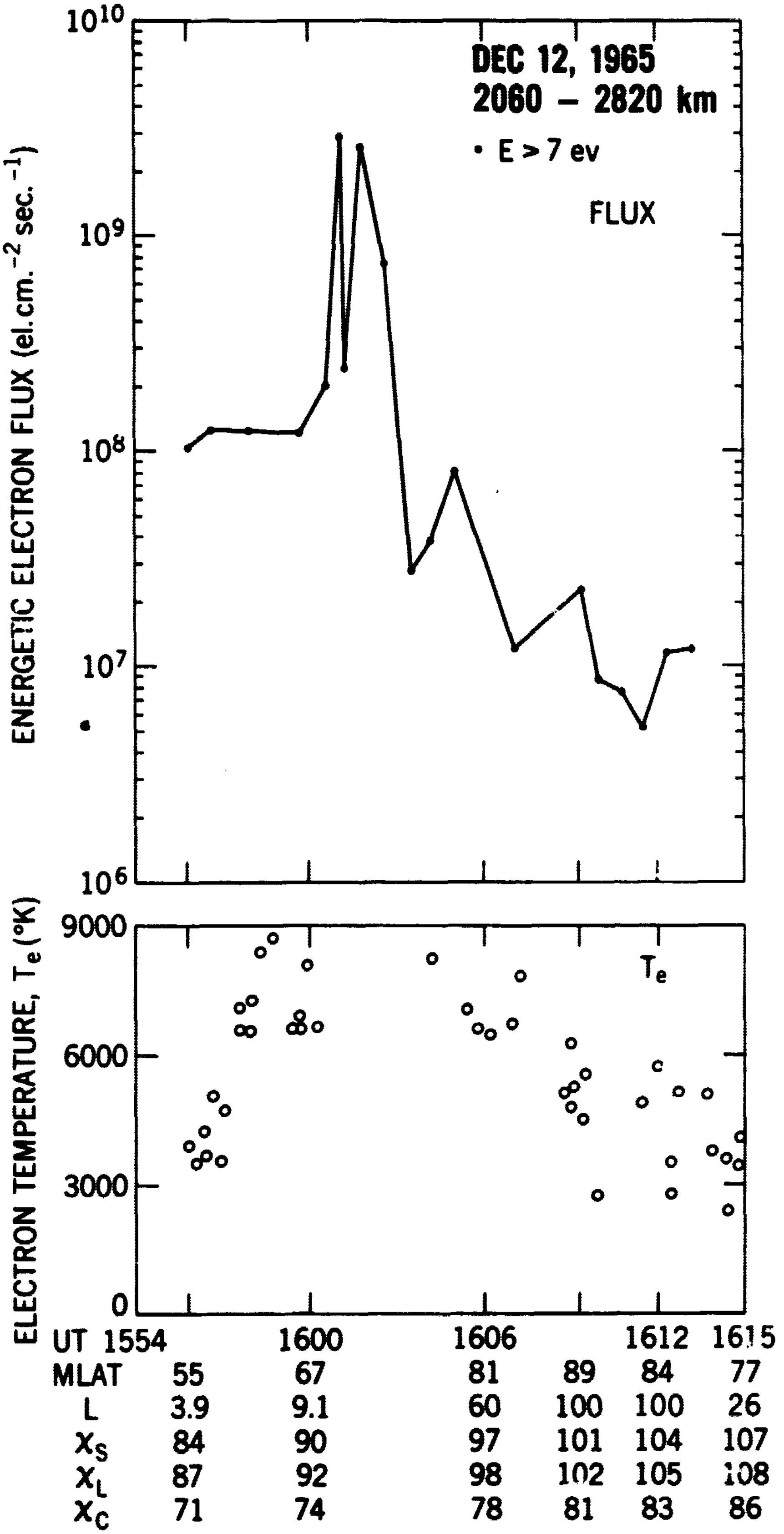
DEC 12, 1965
2060 – 2820 km
• E > 7 ev
FLUX
ENERGETIC ELECTRON FLUX (el.cm.$^{-2}$sec.$^{-1}$)
10^{10}
10^{9}
10^{8}
10^{7}
10^{6}
ELECTRON TEMPERATURE, T_e (°K)
T_e
9000
6000
3000
0
UT 1554 1600 1606 1612 1615
MLAT 55 67 81 89 84 77
L 3.9 9.1 60 100 100 26
X_S 84 90 97 101 104 107
X_L 87 92 98 102 105 108
X_C 71 74 78 81 83 86

Figure 7